

Low velocity impact behavior of auxetic CFRP composite laminates with in-plane negative Poisson's ratio

Journal of Composite Materials
2023, Vol. 57(12) 2029–2041
© The Author(s) 2023
Article reuse guidelines:
sagepub.com/journals-permissions
DOI: 10.1177/00219983231168698
journals.sagepub.com/home/jcm


Wenhua Lin  and Yeqing Wang 

Abstract

Introducing auxeticity or negative Poisson's ratio is one potential solution to mitigate the low velocity impact damage of fiber reinforced polymer matrix composites, which can be achieved by tailoring the layup of an anisotropic composite laminate. This study aims to investigate the effect of laminate-level in-plane negative Poisson's ratio on the low velocity impact behavior of carbon fiber reinforced polymer (CFRP) matrix composites using numerical simulations. The layups of the auxetic composites that allow them to produce negative Poisson's ratios are identified based on the Classical Lamination Theory and verified through fundamental coupon-level experimental tests. To ensure meaningful comparisons, the non-auxetic counterpart composites are designed by allowing them to produce positive in-plane Poisson's ratio while closely matching the longitudinal effective modulus of the auxetic laminate. The simulation results indicate that the auxetic laminates suffer smaller (12.6% on average) delamination area in top and bottom interfaces, much smaller (38% on average) matrix compressive damage in the top and bottom plies, and smaller (14.6% on average) fiber tensile damage area in each ply of the laminate at relatively higher impact energies (5 and 8 J).

Keywords

carbon fiber composite laminates, negative poisson's ratio, auxetic composites, low velocity impact, numerical simulations

Introduction

Carbon fiber reinforced polymer (CFRP) matrix composites, owing to their superior properties, such as high specific stiffness and specific strength, excellent fatigue and corrosion resistance, and low coefficient of thermal expansion, have continuously gained interests across various industries including aerospace, marine, automotive, energy, civil infrastructure, and high-end sports. However, CFRP composites are not without their drawbacks, one of which is the susceptibility to low velocity impact damage which, for aircraft, can be results of tool drop, runway debris, and bird strike during takeoff and landing.^{1,2} These impact events could lead to external and internal damages of a CFRP composite structure in various damage modes, such as fiber breakage, delamination, matrix cracking, which will significantly compromise the structural integrity.^{3–6}

One solution to mitigate the low velocity impact damages of CFRP composites is to introduce laminate-level auxeticity or negative Poisson's ratio into the composite structure,^{7–11} which can be achieved by varying the individual constituent lamina orientations of a CFRP composite.¹² For instance, works of Aziz¹³ investigated the effect of in-plane negative Poisson's ratio on the indentation

and low velocity impact responses of IM7/8552 CFRP composites with specially designed layup orientations to produce in-plane Poisson's ratios of -0.134 and 0.446 , with closely matched tensile modulus. The low velocity impact tests revealed that the damage for CFRP laminates with the in-plane negative Poisson's ratio was localized and directly under the impactor nose region with smaller extents of delamination. Moreover, the peak load and energy absorbed were found to be consistently higher at all impact energies of 3.15, 12.1, and 31.4 J. Results from the quasi-static indentation tests showed a 19% increase in peak load and 27% increase in energy absorbed, and a 29% reduction in the extent of damage for CFRP laminates with an in-plane negative Poisson's ratio of -0.134 .

Despite the existing experimental evidence of improved impact resistance of CFRP composites with a negative

Department of Mechanical and Aerospace Engineering, Syracuse University, Syracuse, NY, USA

Corresponding author:

Yeqing Wang, Department of Mechanical and Aerospace Engineering, Syracuse University, 130 Sims Drive, 223 Link Hall, Syracuse, NY, USA.
Email: ywang261@syr.edu

Poisson's ratio, the underlying damage mechanism of such enhancement remain to be explored. To investigate the dynamic impact response of CFRP composites, many researchers have favored numerical simulation methods over experimental testing since: i) it can be costly and time-consuming to perform experimental tests on CFRP composites given the high material and equipment costs and long processing times, ii) it can be difficult to capture the progressive damage developments of CFRP composites during an impact event, especially during low velocity impact tests where the damages could be barely visible at low impact energy levels, and that the instantaneous dynamic response of the impact can be over within the magnitude of several milliseconds. Many studies have been conducted by researchers worldwide to investigate the low velocity impact response of CFRP composites using numerical simulation methods where the failure modes of CFRP composites can be categorized into interlaminar damage and intralaminar damage and can be simulated by exploiting various combinations of damage initiation criteria and damage progression methods.^{6,14–27} The aim of this study is to utilize the well-validated, state-of-the-art, numerical simulation methods to explore the underlying mechanisms of enhancement of impact resistance imparted by the introduction of in-plane negative Poisson's ratio into CFRP composites.

In the current work, laminate layup schedules were identified based on the classical lamination theory (CLT) to produce both CFRP composites with in-plane auxetic behavior, and counterpart CFRP composite with non-auxetic behavior. Two matching configurations were used to select the layup schedules of non-auxetic CFRP composites where Configuration 1 closely matched the effective longitudinal modulus with extremely tight tolerance to that of the auxetic CFRP and Configuration 2 matched effective moduli in all three principal directions with relatively higher tolerance. These identified layup schedules were then used in low velocity impact modeling of CFRP composites implemented with finite element analysis.

Layups of CFRP composite laminates that allow to produce negative Poisson's ratios

Laminate-level (or effective) negative Poisson's ratio can be achieved by manipulating the individual constituent lamina layup orientations which determines the anisotropy of individual lamina and the strain mismatch between adjacent plies. It can be expressed in terms of the \mathbf{J} matrix, which is derived based on the CLT in functions of the \mathbf{A} , \mathbf{B} , and \mathbf{D} stiffness matrices. The detailed derivations can be found in author's previous works.^{28,29} The final expression for the laminate-level in-plane Poisson's ratio, ν_{12}^e , is shown below,

$$\nu_{12}^e = -\frac{J_{21}}{J_{11}}, \quad (1)$$

where J_{11} and J_{21} are elements of the \mathbf{J} matrix,

$$\mathbf{J} = \mathbf{A}^{-1} + \mathbf{A}^{-1}\mathbf{B}(\mathbf{D} - \mathbf{B}\mathbf{A}^{-1}\mathbf{B})^{-1}\mathbf{B}\mathbf{A}^{-1}, \quad (2)$$

where \mathbf{A} , \mathbf{B} , and \mathbf{D} are the extensional stiffness matrix, extensional-bending coupling stiffness matrix, and bending stiffness matrix according to the CLT.

A MATLAB code was developed based on the above expressions to identify laminate layup schedules that allow the laminate to produce negative in-plane Poisson's ratio. The engineering constants of the IM7/977-3 CFRP composite lamina^{14,15,30} used for calculating the \mathbf{A} , \mathbf{B} and \mathbf{D} matrices is shown in Table 1. Figure 1 shows the calculation results for the in-plane Poisson's ratio, ν_{12}^e , given the specified laminate layup schedule of $[\theta_2/65_2/\theta_2/65_2/\theta_2]$ while the ply angle, θ , is allowed to vary within ranges of 0–90 degrees. It can be seen that the negative in-plane Poisson's ratio can be produced when the ply angle is between 5 and 40 degrees and that the highest negative in-plane Poisson's ratio is obtained when the ply angle is 15 degrees with the restriction of fixed ply angle of 65 degrees in plies 2 and 4.

Layups of non-auxetic CFRP counterpart laminates with positive Poisson's ratios

It is very important to note that there is a “side effect” associated with tuning the laminate layup schedule to produce the negative Poisson's ratio, that is the simultaneous change of the effective moduli of the laminate.⁷ Therefore, to ensure that the change in the low velocity impact behavior is caused by the auxeticity and not due to the change of the effective moduli, it is important to properly choose the counterpart CFRP laminates for meaningful comparisons. Thus, the layup schedules of the counterpart CFRP laminates are identified such that the laminates exhibit positive in-plane Poisson's ratio and at the same time have similar if not identical effective moduli to those of the auxetic laminates, where the well-validated method proposed by Sun and Li³¹ are used to calculate the effective moduli of the laminates. Note that there exist no layup schedules that would produce non-auxetic counterpart laminates that have identical effective moduli in all three principal directions (i.e., E_1^{eff} , E_2^{eff} , and E_3^{eff}) to those of the auxetic composite laminate at the same time. Therefore, two matching configurations were used to identify layup schedules of the non-auxetic counterpart laminates, of which Configuration 1 strictly matches the longitudinal effective modulus, E_1^{eff} , with extremely low tolerance and through-thickness modulus, E_3^{eff} , with intermediate tolerance, and high tolerance on the transverse effective modulus

Table 1. Material properties of IM7/977-3 CFRP composites.^{14,15,30}

	Density	$\rho = 1600 \text{ kg/m}^3$
Composite lamina properties	Elastic moduli	$E_{11} = 159 \text{ GPa}, E_{22} = E_{33} = 9.2 \text{ GPa}$ $G_{12} = G_{13} = 4.37 \text{ GPa}, G_{23} = 2.57 \text{ GPa}$
	Poisson's ratio	$\nu_{12} = \nu_{13} = 0.253, \nu_{23} = 0.456$
	Strength	$X_T = 2275 \text{ MPa}, X_C = 1680 \text{ MPa},$ $Y_T = 64 \text{ MPa}, Y_C = 168 \text{ MPa}.$
	Fracture actenergy	$S_{xy} = 121 \text{ MPa}, S_{yz} = S_{zx} = 127 \text{ MPa}$ $G_{ft} = 133 \text{ N/mm}, G_{fc} = 40 \text{ N/mm}$ $G_{mt} = 0.6 \text{ N/mm}, G_{mc} = 2.1 \text{ N/mm}$
Interface properties	Modulus	$E = 5 \text{ GPa}$
	Strength	$N = S = 30 \text{ MPa}$
	Fracture energy	$G_n^C = 0.6 \text{ N/mm (normal)}, G_s^C = 2.1 \text{ N/mm (shear)}$

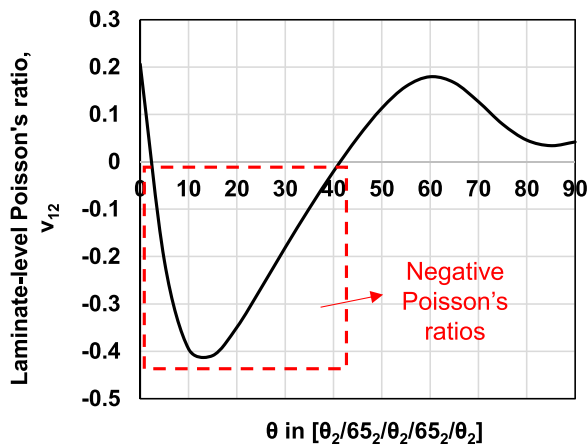


Figure 1. Predicted layups to produce laminate-level in-plane negative Poisson's ratios in IM7/977-3 CFRP composite laminate with a layup of $[\theta_2/65_2/\theta_2/65_2/\theta_2]$ as the ply angle, θ , changes from 0 to 90 degrees.

(E_2^{eff}). Whereas Configuration 2 identifies the best layup schedule available that matches all three effective moduli at the same time with relatively higher tolerance.

Table 2 shows the layup schedules and the effective tensile and shear moduli of the non-auxetic counterpart composite laminate identified based on Configurations 1 and 2 and the tolerances calculated for each effective modulus, where the tolerance here refers to the percentage difference between the modulus of the auxetic laminate and the modulus of the non-auxetic counterpart laminate in corresponding directions. By considering the two configurations of the non-auxetic laminates, both the effect of negative Poisson's ratio and the coupling effects between the negative Poisson's ratio and the effective moduli, in particularly the transverse effective modulus, E_2^{eff} , can be investigated. Figure 2 shows a schematic of the layup orientations identified for the auxetic and non-auxetic 1 and 2 configurations. These laminate layup schedules that produce in-plane auxetic and non-auxetic laminates will be used in the numerical studies described in Section 5 to

investigate the effect of in-plane negative Poisson's ratio on the low velocity impact behavior of CFRP laminates. To briefly mention again, the layup schedule of the auxetic laminate is chosen to be $[15_2/65_2/15_2/65_2/15_2]$ since it produces the highest negative in-plane Poisson's ratio as can be seen in Figure 1, which is expected to provide the most significant enhancement in the low velocity impact resistance.

Table 3 shows the results of the in-plane Poisson's ratio and the laminate-level longitudinal effective modulus for the auxetic and the non-auxetic Configuration 1 CFRP laminates obtained through fundamental coupon-level tensile tests in our prior work.³² The results showed good agreement between the predicted and measured values where the in-plane Poisson's ratio was measured to be -0.41 with a standard deviation of 0.0117 and 0.159 with a standard deviation of 0.0048 , and the longitudinal effective modulus was measured to be 52.14 GPa with a standard deviation of 0.896 GPa and 52.12 GPa with a standard deviation of 0.774 GPa for the auxetic and non-auxetic Configuration 1 CFRP laminates, respectively.

Low velocity impact model for CFRP composite laminates

To study the effect of negative Poisson's ratios on the low velocity impact behaviors of the composite laminates, a well-validated impact damage modeling approach is used.^{6,14–21,33–42} The detailed modeling approach, including the choices of the damage initiation criteria, the damage evolution law, the degradation of the stiffness matrix, and the delamination model, have been well discussed and presented in numerous existing papers^{6,15,17} and are omitted here for brevity. The primary components of the low velocity impact model adopted throughout this study include: 1) the Hashin damage criterion, which is used to predict the initiation of the fiber tensile and compressive failure and the matrix tensile and

Table 2. Layups and effective tensile and shear moduli of the auxetic laminate and the corresponding non-auxetic counterpart composite laminates in two configurations.

	In-plane auxetic CFRP laminate	Configuration 1: Non-auxetic counterpart CFRP laminate (with strictly matched E_1^{eff} and E_3^{eff})	Configuration 2: Non-auxetic counterpart CFRP laminate (with weakly matched E_1^{eff} , E_2^{eff} , and E_3^{eff})
Layup	[15 ₂ /65 ₂ /15 ₂ /65 ₂ /15 ₂]	[35 ₂ /60 ₂ /-5 ₂ /60 ₂ /35 ₂]	[40 ₂ /65 ₂ /0 ₂ /65 ₂ /40 ₂]
ν_{12}^e	-0.409	0.160	0.020
E_1^{eff} (GPa)	51.29	51.29 (+0.013%)	45.33 (-11.6%)
E_2^{eff} (GPa)	25.53	21.03 (-17.6%)	25.23 (-1.2%)
E_3^{eff} (GPa)	9.95	10.26 (+3.1%)	10.26 (+3.1%)
G_{12}^{eff} (GPa)	6.16	11.02 (+78.9%)	9.86 (+60.1%)
G_{13}^{eff} (GPa)	3.47	3.35 (-3.5%)	3.25 (-6.3%)
G_{23}^{eff} (GPa)	3.03	3.13 (+3.3%)	3.23 (+6.6%)

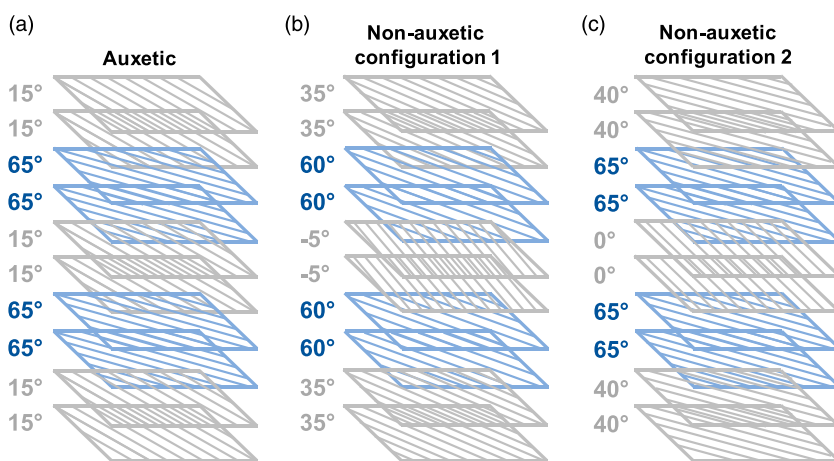


Figure 2. Schematic of layup orientations for the (a) auxetic laminate, (b) non-auxetic configuration 1 laminate, and (c) non-auxetic configuration 2 laminate.

Table 3. Predicted and experimentally measured mechanical properties of auxetic and non-auxetic Configuration 1 CFRP laminates.

	In-plane auxetic CFRP laminate	Configuration 1: Non-auxetic counterpart CFRP laminate
Layup	[15 ₂ /65 ₂ /15 ₂ /65 ₂ /15 ₂]	[35 ₂ /60 ₂ /-5 ₂ /60 ₂ /35 ₂]
ν_{12}^e predicted	-0.409	0.160
ν_{12}^e experimental	-0.410 ± 0.0117	0.159 ± 0.0048
E_1^{eff} predicted (GPa)	51.29	51.29
E_1^{eff} experimental (GPa)	52.14 ± 0.896	52.12 ± 0.774

compressive failure;⁴³ 2) the linear stiffness degradation function based on the equivalent strain method,¹⁵ which is used to track the damage evolution in each failure mode;¹⁵ and 3) the Benzeggagh and Kenane (B-K) delamination criterion along with mixed-mode fracture energy laws, which are used to model the initiation and evolution of the delamination damage.⁴⁴

In this study, the low velocity impact model is implemented using finite element analysis (FEA) with general purpose FEA software, ABAQUS. Specifically, the above-mentioned stiffness degradation law, damage

initiation, and damage evolution are implemented using a VUMAT subroutine while the delamination damage is modeled by defining cohesive surface contacts between adjacent laminate plies. Such numerical implementations are also well described in many existing papers.^{6,15,18} The VUMAT subroutine is available from the corresponding author upon request.

Before the model is used to study the effect of the negative Poisson’s ratio, it was verified using a benchmark low velocity impact problem reported by ref.¹⁸ The comparison between the experimental results reported in ref.¹⁸

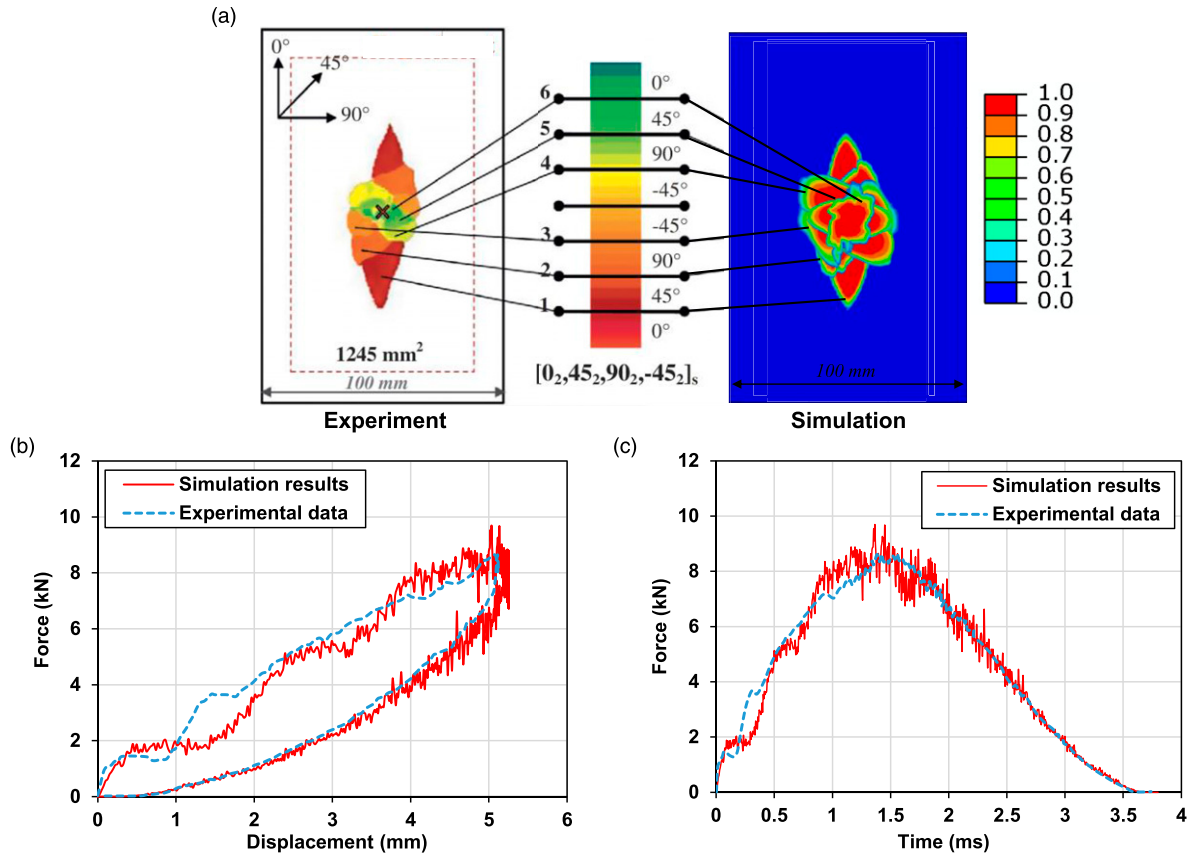


Figure 3. Comparison between the experimental (data from ref. ¹⁸) and simulation results at impact energy of 25 J for model verification: (a) comparison of stacked delamination areas between experimental data obtained through C-scan reported in ref. ¹⁸ and simulation, (b) force displacement plot, (c) force history plot.

and our simulation results is shown in Figure 3. Specifically, Figure 3(a) shows the comparison between the stacked delamination areas obtained using C-scan (left figure) reported in ref. ¹⁸ and our simulation results (right figure). The color legend for the C-scan represents the location of the delamination along the thickness direction, where the green color represents the delamination at the top interface while the red color represents the delamination at the bottom interface. The color legend for our simulation indicates the degree of delamination, where the red color represents a complete delamination while the blue color represents no delamination. The overall delamination patterns predicted are found to be in good agreement with the experimental data. The force displacement and force history plots shown in Figure 3(b) and (c) also show good agreement between our simulation results and the reported experimental data. Further details of the model verification can be found in our prior work. ⁴⁵ Figure 4 shows the schematic of the problem setup which consists of the CFRP laminate with a dimension of $150 \times 100 \times 4.16$ mm, the impactor which is made of steel and has a semi-spherical shape with a diameter of 16 mm and a velocity of 5 m/s that represents an impact energy of

25 J, and the supporting plate with a dimension of 150×100 mm and a cutout window of 125×75 mm at the center that rests the CFRP laminate. The impactor and the supporting plate are modeled as discrete rigid bodies using R3D4 elements, while the CFRP composite laminate is modeled using the C3D8R elements. A global seed sizes of 0.5 mm and 3 mm are defined for the impactor and the supporting plate, respectively. For the CFRP laminate, a refined mesh size of 0.9×0.9 mm is used in a 72×36 mm region located directly under the impactor, whereas the remaining regions are meshed with a global seed size of 3.5 mm to reduce computational time. Moreover, since the layup has paired plies (i.e., adjacent plies with same angles), only one element through the thickness of each paired ply was created to further reduce the computational time. The meshing leads to a total of 85625 elements. To model the delamination, the interfaces between each adjacent ply pairs are assigned using cohesive surface contacts. The layups of the laminates follow those identified in Table 2. The material properties used in the simulation studies are shown in Table 1. The simulations were conducted at three elevated impact energy levels, i.e., 3, 5, and 8 J. The choice of these

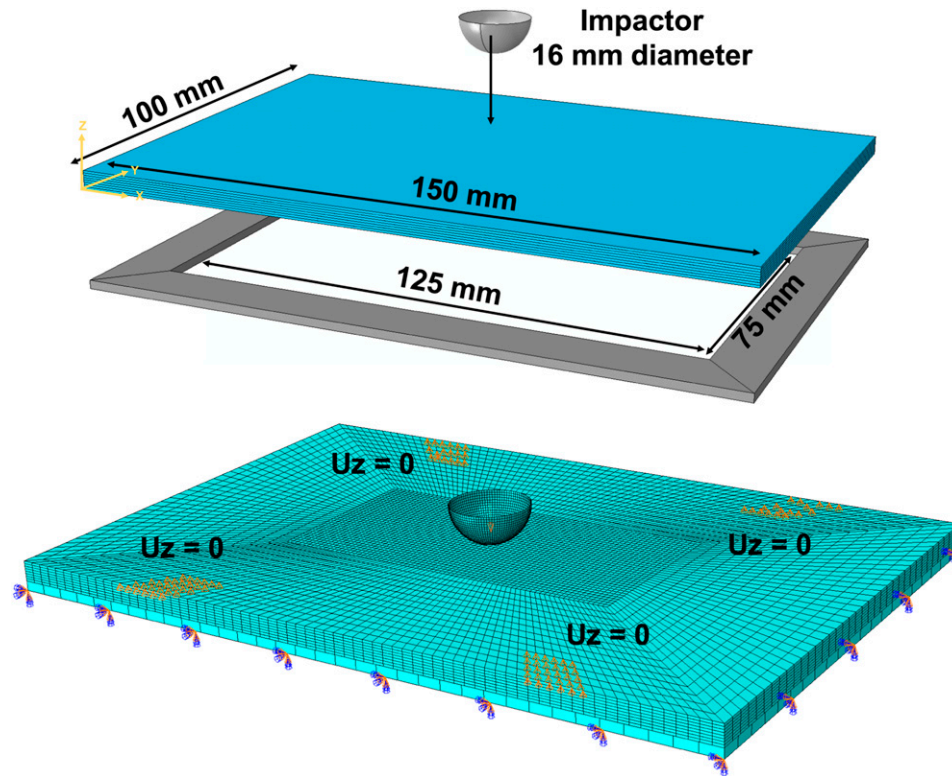


Figure 4. Low velocity impact model setup for finite element analysis.

three energy levels is because they were found, from preliminary trial-and-error simulation studies, to produce minimum, intermediate, and maximum damage without causing the laminates to penetrate.

Results and discussions

Figure 5 shows the comparison of the global impact response between the in-plane auxetic and the corresponding non-auxetic CFRP composite laminates at 3, 5, and 8 J. For the impact force shown in Figure 5(a), no consistent pattern can be identified regarding the role of the in-plane negative Poisson's ratio in influencing the impact force. It can be observed that, although the auxetic laminate has a higher transverse effective modulus in comparison to the non-auxetic Configuration 1 laminate, the impact force at 3 J is still 10.5% lower. As the impact energy increases to 5 and 8 J, the impact forces become higher than those of the non-auxetic Configuration 1 laminate, which are consistent with findings reported by Aziz.¹³ When compared to the non-auxetic Configuration 2 laminate, the auxetic laminate shows lower impact forces at 3 and 5 J and a slightly higher impact force when the impact energy increases to 8 J. Overall, the results show that the auxetic laminate exhibits a higher increase rate of the impact force than the non-auxetic laminates as the impact energy increases. This

is closely related to the damage behaviors during the impact and is discussed in the following sections.

The effects of the in-plane negative Poisson's ratio on the impact time, maximum displacement, and the dissipated energy are illustrated in Figure 5(b)–(d). The results of the impact time and the dissipated energy share one similarity (see Figures 5(b) and 5(d)), that is, at 3 J, the auxetic laminate shows a higher impact time and a higher dissipated energy than the non-auxetic laminates, but, when the impact energy increases to 8 J, an opposite pattern can be observed, where the impact time and the dissipated energy of the auxetic laminate become much lower than those of the non-auxetic laminates. Specifically, at 8 J, the impact time is 12.0% and 6.0% lower than that of the non-auxetic Configurations 1 and 2, respectively. For the dissipated energy, at a lower impact energy of 3 J, the dissipated energy for the auxetic laminate is 16.6% and 48.9% higher than that for non-auxetic Configurations 1 and 2, respectively. While at higher impact energies, the dissipated energy of the auxetic laminate is 27.3% and 1.8% lower than the non-auxetic configurations at 5 J, and 20.4% and 16.1% lower than the non-auxetic configurations at 8 J. This finding may suggest that the in-plane auxetic laminate has lower increase rates of the impact time and dissipated energy than the non-auxetic laminates as the impact energy increases. For the maximum displacement during the impact, as

shown in Figure 5(c), the effect of the in-plane negative Poisson's ratio is insignificant.

Effect on the delamination damage

A comparison of the predicted delamination patterns in each interface of the in-plane auxetic laminate and the

corresponding non-auxetic laminates is provided in Figure 6. The delamination propagation is approximately parallel to the fiber orientations of the ply below the corresponding interface, except for the bottom interface. This is consistent with findings reported by refs.^{15,46} Overall, no clear role of the in-plane negative Poisson's ratio in influencing the shapes of the delamination areas can be identified.

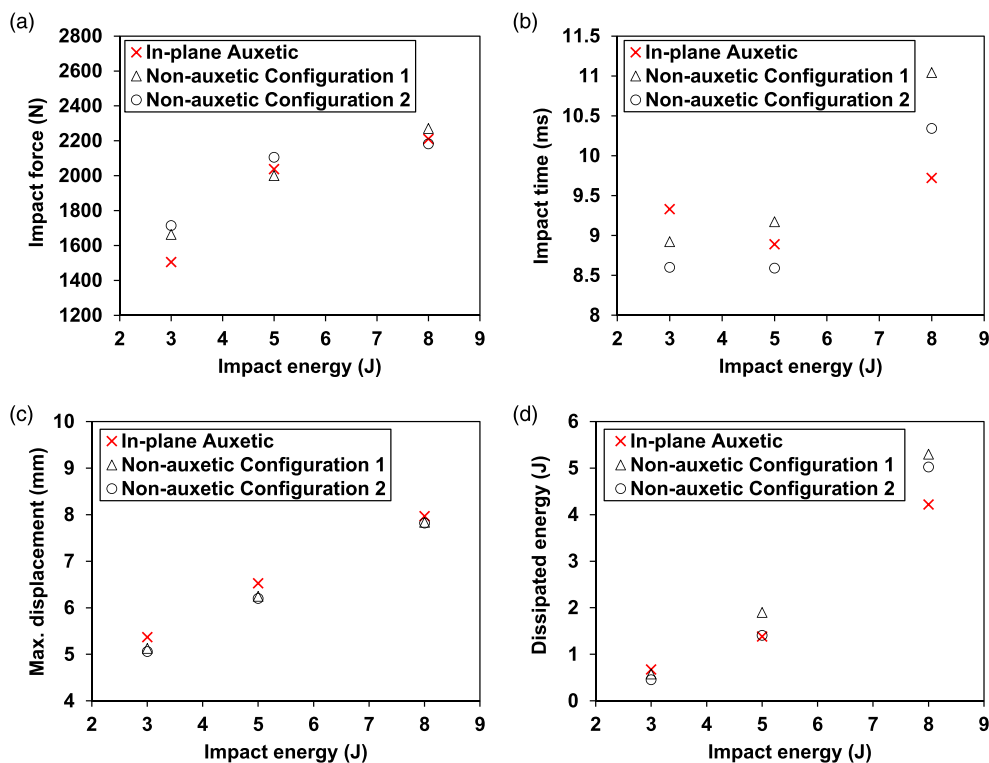


Figure 5. Predicted parameters reflecting the global response of the in-plane auxetic and corresponding non-auxetic CFRP composite laminates during low velocity impact: (a) impact load, (b) impact time, (c) maximum displacement, and (d) dissipated energy.

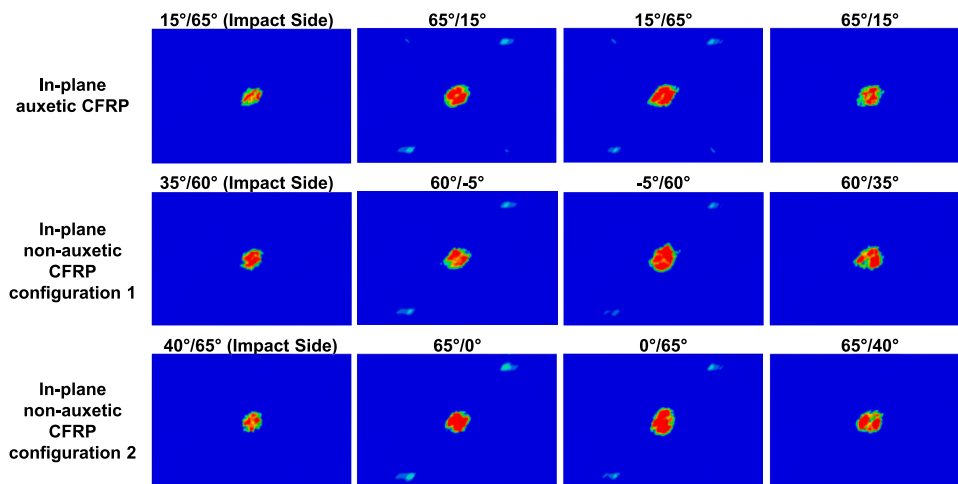


Figure 6. Comparison of predicted delamination damage patterns in each interface of the in-plane auxetic CFRP laminate and the corresponding non-auxetic laminates, subjected to an impact energy of 8 J.

To further examine the effect of the in-plane negative Poisson’s ratio on the delamination damage, the quantitative comparison of the predicted delamination area in each interface of the auxetic and non-auxetic laminates is plotted in Figure 7. As shown in Figure 6, regions with dark blue color represent no delamination damage and regions with red color represent complete delamination damage. The delamination areas are obtained using the imageJ software by measuring the areas with colors other than the dark blue. Same methods are used for obtaining the quantitative damaged areas from the contour plots of the fiber and matrix damage in following discussions. The top and bottom

interfaces of the auxetic laminates exhibit generally lower delamination areas than those of the two non-auxetic laminates at three impact energy levels, with one exception for the case at the bottom interface at 3 J. At 8 J, the reductions of the delamination areas are 17.0% and 13.7% at the top and bottom interfaces, respectively, in comparison to those of the non-auxetic Configuration 1 laminate, while the reductions are 9.9% and 9.8%, respectively, in comparison to those of the non-auxetic Configuration 2 laminate. Unlike the top and bottom interfaces, the middle two interfaces exhibit delamination areas in between those of the two non-auxetic laminates at 3 and 5 J. At 8 J, the auxetic laminate

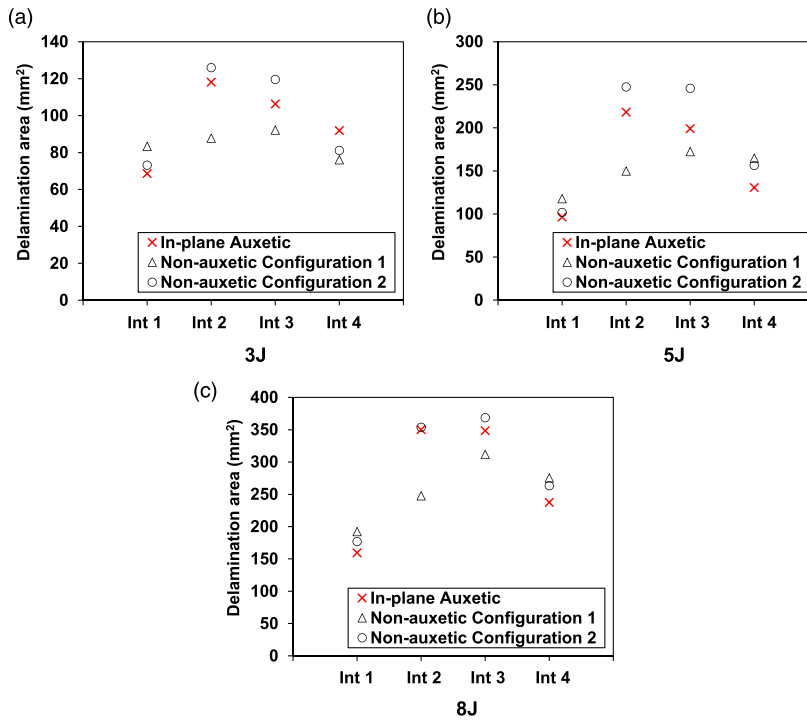


Figure 7. Comparison of the predicted delamination area in each interface of the in-plane auxetic and corresponding non-auxetic CFRP composite laminates at different impact energies: (a) 3 J, (b) 5 J, and (c) 8 J, where “int” in the horizontal axis denotes interface.

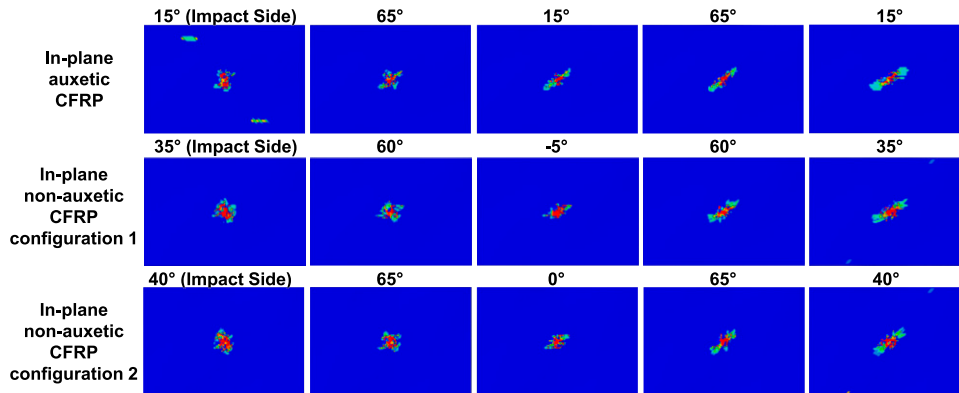


Figure 8. Comparison of predicted matrix tensile damage in each ply of the in-plane auxetic CFRP laminate and corresponding non-auxetic laminates, subjected to an impact energy of 8 J.

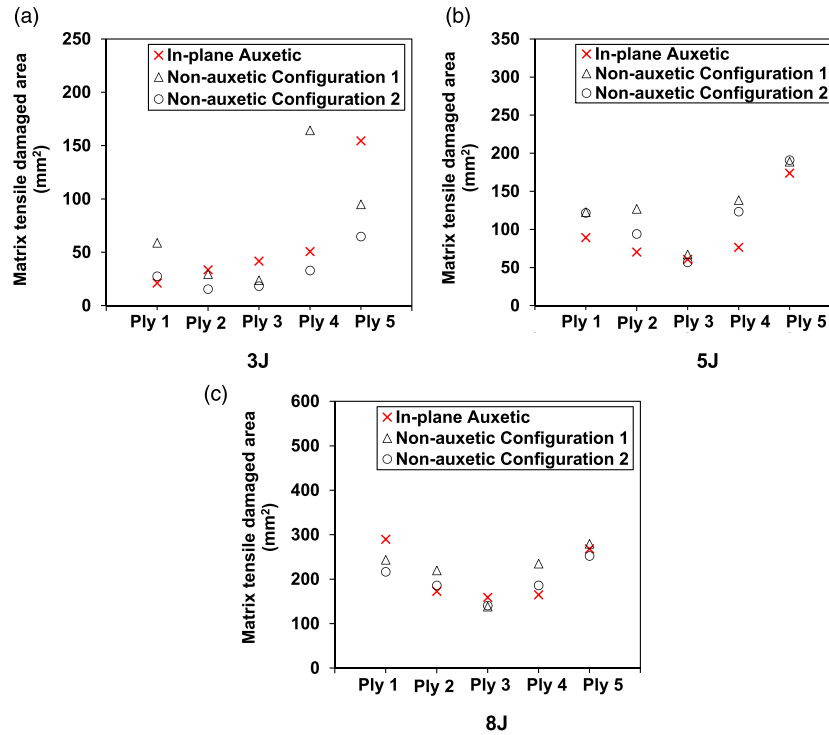


Figure 9. Comparison of the predicted matrix tensile damaged area in each ply of the in-plane auxetic CFRP laminate and non-auxetic laminates at different impact energies: (a) 3 J, (b) 5 J, and (c) 8 J.

shows almost identical delamination areas to those of the two non-auxetic laminates. The results suggest that producing the in-plane negative Poisson's ratio is beneficial for reducing the delamination areas at the top and bottom interfaces, especially at relatively higher impact energies.

Figure 8 shows the comparison of matrix tensile damage patterns in the in-plane auxetic laminate and the corresponding non-auxetic laminates at an impact energy of 8 J. As one can see, the patterns of the damaged areas are similar in the auxetic and non-auxetic laminates, where the top two plies exhibit localized damage, while the back three plies show damage propagations along the fiber direction. Such matrix tensile damage patterns are common for CFRP composites under low velocity impact.¹⁵ No apparent effect of the in-plane negative Poisson's ratio on the patterns of the matrix tensile damage can be identified.

A quantitative comparison of the matrix tensile damaged area in each ply of the in-plane auxetic laminate and the corresponding non-auxetic laminates at three impact energy levels is provided in Figure 9. For the non-auxetic Configuration 1 laminate, one consistent pattern can be observed where the lowest matrix tensile damaged areas are found to be at ply three at all energy levels, whereas the largest matrix tensile damaged area is found to be at ply four for impact energy of 3 J, and at ply five for impact energy of 5 and 8 J. For the

non-auxetic Configuration 2 laminate, the distribution of the matrix tensile damaged areas in the five plies shows a consistent pattern at all energy levels, that is, the damaged area decreases from ply one to ply three where the lowest damaged area is observed and then increases from ply three to ply five, except for the case of 3 J, of which the lowest damaged area is located at ply 2. This pattern is also true for the in-plane auxetic laminate, except for the case at 3 J, where the damaged area continuously increases from the impact side to the back side. This could be due to the unique triaxial state of stresses produced in the auxetic laminate. At 5 J, the in-plane auxetic laminate exhibits generally lower matrix tensile damaged areas than those of the two non-auxetic laminates, except for ply 3, where the damaged area is nearly identical to that of both non-auxetic laminates. At 3 and 8 J, there exists no clear or consistent pattern as of how the in-plane negative Poisson's ratio affects the matrix tensile damaged areas, in comparison to those of the non-auxetic counterparts.

As mentioned in previous studies,^{6,15,20} the fiber tensile damage and matrix compressive damage are comparatively much smaller than the matrix tensile damage. They are negligible at low energy levels at 3 and 5 J. Figure 10 illustrates the comparison of the predicted fiber tensile damage patterns in each ply of the in-plane auxetic laminate and the corresponding two non-auxetic laminates, at an impact

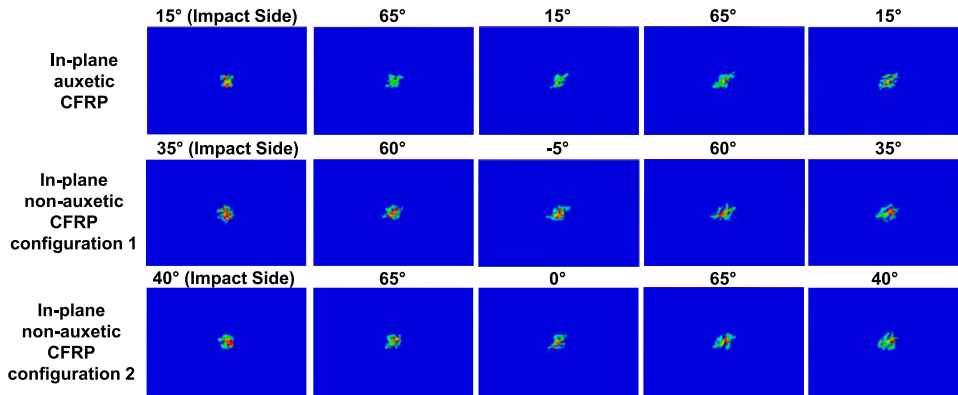


Figure 10. Comparison of predicted fiber tensile damage patterns in each ply of the in-plane auxetic CFRP composite laminate and the corresponding two non-auxetic CFRP composite laminates at an impact energy of 8 J.

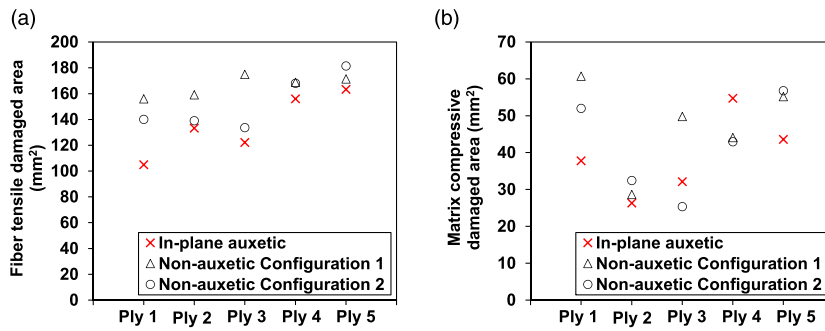


Figure 11. Comparison of the predicted damage areas in each ply of the in-plane auxetic and corresponding non-auxetic CFRP composite laminates at an impact energy of 8 J: (a) fiber tensile damaged area and (b) matrix compressive damaged area.

energy of 8 J. The three laminates all exhibit very localized damage on the impact point, especially in the top two plies and in the bottom ply. Only limited damage has propagated in plies 3 and 4. This finding is consistent for both the auxetic laminate and the non-auxetic laminates. Therefore, the influence of the in-plane negative Poisson’s ratio on the shape of fiber tensile damage is considered insignificant.

Figure 11(a) provides a quantitative comparison of the fiber tensile damaged area in each ply of the in-plane auxetic and the two non-auxetic CFRP laminates at 8 J. The in-plane auxetic laminate exhibits consistently lower damaged area in each ply, when compared to the two non-auxetic laminates. Specifically, the reductions are 32.7%, 16.2%, 30.2%, 7.6%, and 4.7%, in five plies, respectively, in comparison to the non-auxetic Configuration 1 laminate, while the reductions are 25.1%, 4.1%, 8.7%, 7.2%, and 10.0%, in comparison to the non-auxetic Configuration 2 laminate. Recall that the transverse effective modulus of the non-auxetic laminate Configuration 1 is 17.6% lower than that of the auxetic laminate, while the longitudinal effective modulus of the non-auxetic laminate Configuration 2 is 11.6% lower than that of the auxetic laminate. A lower modulus typically delays the

increase of the stresses, which is expected to produce smaller damage based on the Hashin damage criteria. However, in this case, the fiber tensile damaged areas in the two non-auxetic laminates are still higher than those of the auxetic laminate. This indicates that the unique triaxial state of stresses produced in the in-plane auxetic laminate could lead to smaller fiber tensile damage in comparison to the non-auxetic counterparts.

As for the matrix compressive damage, it is relatively much less significant than the other damage modes. Figure 11(b) illustrates the comparison of the predicted matrix compressive damaged area in each ply of the in-plane auxetic laminate and the corresponding non-auxetic laminates. It can be noticed that the auxetic laminate shows much smaller damaged areas in the top two plies and the bottom ply, whereas no clear trend can be found in plies 3 and 4.

To briefly summarize, the simulation results suggest that producing the in-plane negative Poisson’s ratio in the laminate may result in a higher increase rate of the impact force as the impact energy increases. For the damage behaviors, the in-plane negative Poisson’s ratio generally exhibits more influences on the top and bottom plies than the middle plies. Particularly, the results suggest that the

in-plane negative Poisson's ratio contributes to (i) smaller delamination areas in the top and bottom plies, especially at a relatively high impact energy, (ii) smaller matrix tensile damage areas in the top two and bottom two plies at an intermediate impact energy, and (iii) consistently much smaller fiber tensile damage area in each ply of the laminate. In comparison to the effect of the in-plane negative Poisson's ratio, the effect of the out-of-plane negative Poisson's ratio on the low velocity impact damage is quite different, which has been studied in our previous work.⁴⁵ To briefly summarize, the delamination areas for the laminates with out-of-plane negative Poisson's ratio (with a layup of [25₂/-25₂/25₂/-25₂/25₂]) at 8 J impact were found to be 6.5% lower than the non-auxetic configuration 1 laminates (with a layup of [50₂/0₂/50₂/0₂/50₂]), but 107.7% higher than the non-auxetic configuration 2 laminates (with a layup of [20₂/10₂/5₂/10₂/20₂]), on average across four interfaces. Moreover, significantly reduced matrix tensile and fiber tensile damaged areas were found. Specifically, the matrix tensile damaged areas for the auxetic laminates with out-of-plane negative Poisson's ratio were 54.8% and 36.6% lower than the non-auxetic configurations 1 and 2 laminates, while the fiber tensile damaged areas were 43.2% and 41.7% lower than the non-auxetic configurations 1 and 2 laminates, both on average across five plies (adjacent two plies with same angles were treated as one single layer) and at impact energy of 8 J.

Conclusion

The effect of laminate-level in-plane negative Poisson's ratio on the low velocity impact behavior of the CFRP composite laminate is investigated using numerical simulations. The layups of the auxetic laminates (i.e., laminates that produce laminate-level negative Poisson's ratio) are identified based on the Classical Lamination Theory. The identified layup of the in-plane auxetic laminate allows it to produce a ν_{12}^e of -0.409 , which has been verified through fundamental coupon-level tensile tests.

The auxetic laminate with an in-plane negative Poisson's ratio generally exhibit a higher increase rate in the impact force and lower increase rates in the impact time, maximum displacement, and the dissipated energy, as the impact energy increases. However, no consistent effect has been identified on the global impact response at a fixed impact energy level. As for the damage behaviors, the in-plane negative Poisson's ratio contributes to reduced (12.6% on average) delamination areas in the top and bottom interfaces and reduced (38% on average) matrix compressive damaged areas in the top and bottom plies, at relatively higher impact energies (5 and 8 J). No consistent effect has been found on the matrix tensile damage, except that the top two plies and bottom two plies show much reduced matrix tensile damaged area at an impact energy of 5 J. Additionally, the in-plane auxetic laminate also exhibits greatly reduced (14.6% on average) fiber tensile damaged areas.

Declaration of conflicting interests

The author(s) declared no potential conflicts of interest with respect to the research, authorship, and/or publication of this article.

Funding

The author(s) disclosed receipt of the following financial support for the research, authorship, and/or publication of this article: Financial support provided by Syracuse University (SU) and National Science Foundation under Award No. CMMI-2202737.

Data availability statement

The VUMAT subroutine and the datasets generated during and/or analysed during the current study are available from the corresponding author on reasonable request.

ORCID iDs

Yeqing Wang  <https://orcid.org/0000-0002-5673-9897>

Wenhua Lin  <https://orcid.org/0000-0002-5669-7543>

References

1. Berk B, Karakuzu R, Murat Icten B, et al. An experimental and numerical investigation on low velocity impact behavior of composite plates. *Journal of Composite Materials* 2016; 50: 3551–3559.
2. Yalkin HE, Karakuzu R and Alpyıldız T. Experimental and numerical behaviors of GFRP laminates under low velocity impact. *Journal of Composite Materials* 2020; 54: 2999–3007.
3. Hill CB, Wang Y and Zhupanska OI. Effects of carbon nanotube buckypaper layers on the electrical and impact response of IM7/977-3 composite laminates. 27th Annual Technical Conference of the American Society for Composites 2012. Arlington, TX, USA. 1-3 October 2012. pp. 1205–1221.
4. Hill CB, Wang Y and Zhupanska OI. Impact response of CFRP laminates with CNT buckypaper layers. 54th AIAA/ASME/ASCE/AHS/ASC Structures Structural Dynamics, and Materials Conference. Boston, MA, USA. 8-11 April 2013. AIAA 2013-1617.
5. Lin W, Wang Y, Lampkin S, et al. Hail impact testing of stitched carbon fiber epoxy composite laminates. 35th Annual American Society for Composites Technical Conference, Tucson, AZ. 14-17 September 2020
6. Tan W, Falzon BG, Chiu LNS, et al. Predicting low velocity impact damage and compression-After-Impact (CAI) behaviour of composite laminates. *Composites Part A: Applied Science and Manufacturing* 2015; 71: 212–226.
7. Alderson KL and Coenen VL. The low velocity impact response of auxetic carbon fibre laminates. *Phys Stat Sol* 2008; 245: 489–496.

8. Allen T, Shepherd J, Hewage TAM, et al. Low-kinetic energy impact response of auxetic and conventional open-cell polyurethane foams. *Phys Status Solidi B* 2015; 252: 1631–1639.
9. Hou S, Li T, Jia Z, et al. Mechanical properties of sandwich composites with 3d-printed auxetic and non-auxetic lattice cores under low velocity impact. *Materials and Design* 2018; 160: 1305–1321.
10. Li T, Liu F and Wang L. Enhancing indentation and impact resistance in auxetic composite materials. *Composites Part B: Engineering* 2020; 198: 108229.
11. Zhou L, Zeng J, Jiang L, et al. Low-velocity impact properties of 3D auxetic textile composite. *J Mater Sci* 2018; 53: 3899–3914.
12. Evans KE, Donoghue JP and Alderson KL. The design, matching and manufacture of auxetic carbon fibre laminates. *Journal of Composite Materials* 2004; 38: 95–106.
13. Aziz S. *An investigation into the post impact and post indentation behavior of auxetic composites*. Bolton, UK: University of Bolton, 2016.
14. Zhang J and Zhang X. An efficient approach for predicting low-velocity impact force and damage in composite laminates. *Composite Structures* 2015; 130: 85–94.
15. Li X, Ma D, Liu H, et al. Assessment of failure criteria and damage evolution methods for composite laminates under low-velocity impact. *Composite Structures* 2019; 207: 727–739.
16. Pham DC, Lua J, Sun H, et al. A three-dimensional progressive damage model for drop-weight impact and compression after impact. *Journal of Composite Materials* 2020; 54: 449–462.
17. González EV, Maimí P, Camanho PP, et al. Simulation of drop-weight impact and compression after impact tests on composite laminates. *Composite Structures* 2012; 94: 3364–3378.
18. Hongkarnjanakul N, Bouvet C and Rivallant S. Validation of low velocity impact modelling on different stacking sequences of CFRP laminates and influence of fibre failure. *Composite Structures* 2013; 106: 549–559.
19. Qiu A, Fu K, Lin W, et al. Modelling low-speed drop-weight impact on composite laminates. *Materials and Design* 2014; 60: 520–531.
20. Rivallant S, Bouvet C and Hongkarnjanakul N. Failure analysis of CFRP laminates subjected to compression after impact: FE simulation using discrete interface elements. *Composites Part A: Applied Science and Manufacturing* 2013; 55: 83–93.
21. Thorsson SI, Waas AM and Rassaian M. Low-velocity impact predictions of composite laminates using a continuum shell based modeling approach part A: impact study. *International Journal of Solids and Structures* 2018; 155: 185–200.
22. Patnaik G, Kaushik A, Rajput A, et al. Ballistic performance of quasi-isotropic CFRP laminates under low velocity impact. *Journal of Composite Materials* 2021; 55: 3511–3527.
23. Wan Y, Yao J, Li H, et al. Experimental studies of low-velocity impact behavior on hybrid metal wire net/woven carbon-fiber reinforced composite laminates. *Composites Communications* 2022; 32: 101185.
24. Wan Y, Yang B, Jin P, et al. Impact and compression-after-impact behavior of sandwich panel comprised of foam core and wire nets/glass fiber reinforced epoxy hybrid facesheets. *Jnl of Sandwich Structures and Materials* 2021; 23: 2614–2637.
25. Usta F, Türkmen HS and Scarpa F. Low-velocity impact resistance of composite sandwich panels with various types of auxetic and non-auxetic core structures. *Thin-Walled Structures* 2021; 163: 107738.
26. Madke RR and Chowdhury R. Anti-impact behavior of auxetic sandwich structure with braided face sheets and 3D re-entrant cores. *Composite Structures* 2020; 236: 111838.
27. Zhang Y, Cai D, Peng J, et al. On low-velocity impact behavior of sandwich composites with negative Poisson's ratio lattice cores. *Composite Structures* 2022; 299: 116078.
28. Fan Y and Wang Y. A study on effect of auxeticity on impact resistance of carbon nanotube reinforced composite laminates. Proceedings of the American society for composites—thirty-fifth technical conference. USA. 14–17 September 2020.
29. Fan Y and Wang Y. The effect of negative Poisson's ratio on the low-velocity impact response of an auxetic nano-composite laminate beam. *Int J Mech Mater Des* 2021; 17: 153–169.
30. Mohammadi B, Rohanifar M, Salimi-Majd D, et al. Micro-mechanical prediction of damage due to transverse ply cracking under fatigue loading in composite laminates. *Journal of Reinforced Plastics and Composites* 2017; 36: 377–395.
31. Sun CT and Li S. Three-dimensional effective elastic constants for thick laminates. *Journal of Composite Materials* 1988; 22: 629–639.
32. Lin W and Wang Y. Effect of negative Poisson's ratio on the tensile properties of auxetic CFRP composites. 37th American Society for Composites Conference and ASTM D30 Meeting, Tucson, AZ. 19 september 2022. DOI: [10.12783/asc37/36413](https://doi.org/10.12783/asc37/36413)
33. Wang F, Wang B, Kong F, et al. Assessment of degraded stiffness matrices for composite laminates under low-velocity impact based on modified characteristic length model. *Composite Structures* 2021; 272: 114145.
34. Zhou J, Wen P and Wang S. Numerical investigation on the repeated low-velocity impact behavior of composite laminates. *Composites Part B: Engineering* 2020; 185: 107771.
35. Shi Y and Soutis C. Modelling low velocity impact induced damage in composite laminates. *Mech Adv Mater Mod Process* 2017; 3: 12–14.
36. Topac OT, Gozluclu B, Gurses E, et al. Experimental and computational study of the damage process in CFRP composite beams under low-velocity impact. *Composites Part A: Applied Science and Manufacturing* 2017; 92: 167–182.

37. Sun XC and Hallett SR. Barely visible impact damage in scaled composite laminates: experiments and numerical simulations. *International Journal of Impact Engineering* 2017; 109: 178–195.
38. Bouvet C, Rivallant S and Barrau J-J. Low velocity impact modeling in composite laminates capturing permanent indentation. *Composites Science and Technology* 2012; 72: 1977–1988.
39. Tuo H, Lu Z, Ma X, et al. An experimental and numerical investigation on low-velocity impact damage and compression-after-impact behavior of composite laminates. *Composites Part B: Engineering* 2019; 167: 329–341.
40. Lopes CS, Camanho PP, Gürdal Z, et al. Low-velocity impact damage on dispersed stacking sequence laminates. Part II: numerical simulations. *Composites Science and Technology* 2009; 69: 937–947.
41. Farooq U and Myler P. Efficient computational modelling of carbon fibre reinforced laminated composite panels subjected to low velocity drop-weight impact. *Materials and Design (1980-2015)*. 2014;54:43–56.
42. Shi Y, Swait T and Soutis C. Modelling damage evolution in composite laminates subjected to low velocity impact. *Composite Structures* 2012; 94: 2902–2913.
43. Hashin Z. Failure criteria for unidirectional fiber composites. *Journal of Applied Mechanics* 1980; 47: 329–334.
44. Benzeggagh ML and Kenane M. Measurement of mixed-mode delamination fracture toughness of unidirectional glass/epoxy composites with mixed-mode bending apparatus. *Composites Science and Technology* 1996; 56: 439–449.
45. Wang Y. Auxetic composite laminates with through-thickness negative Poisson's ratio for mitigating low velocity impact damage: a numerical study. *Materials* 2022; 15: 6963.
46. Liu PF, Liao BB, Jia LY, et al. Finite element analysis of dynamic progressive failure of carbon fiber composite laminates under low velocity impact. *Composite Structures* 2016; 149: 408–422.